Kallistatin Deficiency Induces the Oxidative Stress-Related Epithelial-Mesenchymal Transition of Retinal Pigment Epithelial Cells: A Novel Protagonist in Age-Related Macular Degeneration

Gang Shen,[1,2] Yanmei Li,[1] Yongcheng Zeng,[1] Fuyan Hong,[1] Jing Zhang,[1] Yan Wang,[1] Chengwei Zhang,[1] Wei Xiang,[1] Jinhong Wang,[1] Zhenzhen Fang,[1] Weiwei Qi,[1] Xia Yang,[1,5] Guoquan Gao,[1,4] and Ti Zhou[1,3,6]

[1]Department of Biochemistry and Molecular Biology, Zhongshan School of Medicine, Sun Yat-Sen University, Guangzhou, China
[2]Department of Laboratory Medicine, Third Affiliated Hospital of Sun Yat-Sen University, Guangzhou, China
[3]Advanced Medical Technology Center, The First Affiliated Hospital, Zhongshan School of Medicine, Sun Yat-Sen University, Guangzhou, China
[4]Guangdong Engineering & Technology Research Center for Gene Manipulation and Biomacromolecular Products, Sun Yat-Sen University, Guangzhou, China
[5]Guangdong Province Key Laboratory of Brain Function and Disease, Zhongshan School of Medicine, Sun Yat-Sen University, Guangzhou, China
[6]China Key Laboratory of Tropical Disease Control (Sun Yat-Sen University), Ministry of Education, Guangzhou, China

Correspondence: Ti Zhou, Department of Biochemistry and Molecular Biology, Zhongshan Medical School, Sun Yat-Sen University, 74 Zhongshan Road II, Guangzhou 510080, China; zhouti2@mail.sysu.edu.cn.

GS and YL contributed equally to this study.

Received: April 3, 2023
Accepted: August 15, 2023
Published: September 8, 2023

Citation: Shen G, Li Y, Zeng Y, et al. Kallistatin deficiency induces the oxidative stress-related epithelial-mesenchymal transition of retinal pigment epithelial cells: A novel protagonist in age-related macular degeneration. *Invest Ophthalmol Vis Sci.* 2023;64(12):15. https://doi.org/10.1167/iovs.64.12.15

Purpose. Retinal pigment epithelium (RPE) dysfunction induced by oxidative stress–related epithelial-mesenchymal transition (EMT) of RPE is the primary underlying mechanism of age-related macular degeneration (AMD). Kallistatin (KAL) is a secreted protein with an antioxidative stress effect. However, the relationship between KAL and EMT in RPE has not been determined. Therefore we aimed to explore the impact and mechanism of KAL in oxidative stress-induced EMT of RPE.

Methods. Sodium iodate (SI) was injected intraperitoneally to construct the AMD rat model and investigate the changes in RPE morphology and KAL expression. KAL knockout rats and KAL transgenic mice were used to explain the effects of KAL on EMT and oxidative stress. In addition, Snail overexpressed adenovirus and si-RNA transfected ARPE19 cells to verify the involvement of Snail in mediating KAL-suppressed EMT of RPE.

Results. AMD rats induced by SI expressed less KAL in the retina, and KAL knockout rats showed RPE dysfunction spontaneously where EMT and reactive oxygen species (ROS) production increased in RPE. In contrast, KAL overexpression attenuated EMT and ROS levels in RPE, even in TGF-β treatment. Mechanistically, Snail reversed the beneficial effect of KAL on EMT and ROS reduction. Moreover, KAL ameliorated SI-induced AMD-like pathological changes.

Conclusions. Our findings demonstrated that KAL inhibits oxidative stress-induced EMT by downregulating the transcription factor Snail. Herein, KAL knockout rats may be an appropriate animal model for observing spontaneous RPE dysfunction for AMD-like retinopathy, and KAL may represent a novel therapeutic target for treating dry AMD.

Keywords: kallistatin, age-related macular degeneration (AMD), epithelial-mesenchymal transition (EMT), retinal pigment epithelium (RPE), snail

Age-related macular degeneration (AMD) is a chronic, progressive disease that may cause vision loss in the aging population.[1] The global average prevalence of AMD is about 8.7%, and it is estimated that up to 288 million persons will have AMD in 2040 globally.[2] Unfortunately, there is currently no treatment for early AMD and late dry AMD. The wet AMD treatment that may stop further vision loss is mainly intravitreal anti-VEGF therapy.[3] However, treatment responses vary, and not all patients achieve or maintain good stable vision in the long term. Even worse, it causes endophthalmitis, retinal detachment, cataract, and increased intraocular pressure.[3] Thus it is urgent to look for better and more effective treatment options for AMD.

Retinal pigment epithelium (RPE) cells are located between the choroid and photoreceptor cells and are

important for maintaining photoreceptor viability and retinal homeostasis.[4] RPE dysfunction is one general feature of AMD.[5] Elevated intracellular oxidative stress and epithelial-mesenchymal transition (EMT) of RPE cells are proposed mechanisms for RPE abnormalities in AMD, including the early and late stages and dry and wet AMD.[6,7] The molecular mechanisms for EMT in AMD are complicated, including signaling pathways and oxidative. TGFβ as the master inducer of EMT, contributed to EMT of RPE,[8] and the TGFβ pathway elevated in the choroidal neovascularization (CNV) and geographic atrophy (GA) data,[9] where epithelial markers like E-cadherin were downregulated and EMT-related transcription factors like Snail and mesenchymal markers were upregulated. Thus RPE cells lose their cell-cell adhesions and apical-basal polarity, transforming into mesenchymal cells, capacitating their migration into the retina and the sub-RPE space via EMT during AMD.[9,10] As previously reported, Snail is a major transcriptional factor during EMT changes of RPE cells in AMD.[11] In addition, oxidative stress contributed to AMD.[12–17] The AMD model induced by sodium iodate (SI) is primarily toxic to the RPE resulting from oxidative stress. Convincing evidence highlights oxidative stress caused by the increased intracellular levels of reactive oxygen species (ROS) as crucial conspirators in EMT engagement.[18,19] Encoded by SOD2, manganese superoxide dismutase (MnSOD) is an essential molecule against oxidative stress. Mice with SOD2 gene knockout exhibit pathological features similar to AMD patients, and early injection of AAV-SOD2 can prevent dry AMD.[20–22] Furthermore, our recent study has shown that the Snail-MnSOD axis formed a mutual loop via regulating EMT and ROS levels in RPE cells.[23]

Kallistatin (KAL) is a serine proteinase inhibitor (serpin) family member.[24] Kallistatin acts as an antioxidant to protect against oran injury by blocking TNF-α and TGF-β signaling and stimulating eNOS and SIRT1 expression, leading to NADPH oxidase inactivation and SOD2 activated, finally reducing ROS level and relieving oxidative stress.[25] However, the role of KAL in the EMT of RPE remains unknown. Therefore we speculate that KAL may suppress EMT by reducing oxidative stress. In this study, we intend to illuminate the effect and potential mechanism of KAL on the EMT of RPE cells during AMD.

Material and Methods

Animals

The animal research was approved by the Ethical Committee of Animal Research of Sun Yat-Sen University in accordance with the ARVO Statement for the Use of Animals in Ophthalmic and Vision Research. All animals were raised in SPF conditions. A human KAL transgenic C57BL/6J mouse (KAL-TG) strain was gifted by Dr. Jianxing Ma Laboratory at the University of Oklahoma.[26] Sprague-Dawley (SD) rats heterozygous for the deleted KAL were constructed by Cyagen (Guangzhou, China) using CRISPR/Cas9 technology. We considered only the homozygous KAL knockout as KAL-KO rat models and wild-type (WT) SD rats as controls. We administered SI at 35 mg/kg (body weight) into six-month-old C57BL/6J mice or SD rats intraperitoneally to construct a human-like AMD model. Mice or rats were injected intraperitoneally with an equivalent dose of normal saline solution as controls. All tests were performed with male mice or rats unless otherwise indicated.

Fundus Photograph and Ocular Coherence Tomography (OCT)

After animals were anesthetized and pupils dilated, color fundus photography was performed on a fundus imaging system (MicronIV, Phoenix, AZ, USA), and OCT was measured by a system (SpectralisOCT, Heidelberg, Germany). In the OCT test, the mean total retina was measured within a 3 mm circle and line in radius from the optical nerve head, overlapping 100 pictures each time.

Western Blot

Equal amounts of protein were measured, separated by 10% SDS-PAGE, and transferred onto a polyvinylidene fluoride (PVDF) membrane. PVDF membranes were incubated in 5% nonfat dry milk at room temperature for one hour, followed by incubation with primary antibodies overnight, washed by 1 × Tris Buffered Saline (TBS) with 0.1% Tween (TBST) for 10 minutes three times, then removed the TBST and incubated with secondary antibodies for four hours at 4°C. Chemiluminescence was developed using enhanced chemiluminescence (ECL) substrate and detected by a chemiluminescence imaging system (ChemiDoc Touch; Bio-Rad Life Science, Hercules, CA, USA). Antibodies used here are listed in Supplementary Table S1.

Histological Analyses

Frozen retinal sections were thawed for up to 15 minutes at room temperature and washed in PBST (PBS with 0.1% Tween) three times for five minutes each. Then the sections were blocked with goat serum for one hour and incubated at 4°C overnight with primary antibodies. After being washed in PBST three times for five minutes, sections were incubated with fluorescent secondary antibodies for one hour at 37°C. Last, after being washed in PBST three times for five minutes, the sections were stained with 0.5 µg/mL DAPI dilution 1:1000 in PBS for 10 minutes at 37°C. Antibodies used here are listed in Supplementary Table S1. In addition, paraffin-embedded tissue sections were stained with hematoxylin-eosin (H&E) and Masson to determine the retina tissue morphology and collagen volume fraction. All images were captured using an automatic digital slide scanning system (AxioScan.Z1; Zeiss, Oberkochen, Germany).

Cells

Human RPE cell line ARPE19 (ATCC, Manassas, VA, USA) was cultured with 10% fetal bovine serum (FBS) (Gibco, Thermo Fisher Scientific, Waltham, MA, USA) Dulbecco's modified Eagle's medium (DMEM) (Invitrogen, Carlsbad, CA, USA) in an incubator at 5% CO_2 and 37°C. Primary RPE cells were isolated and purified from the eyes of WT or KAL-KO SD suckling rats at two weeks. After the cornea, lens, vitreous, and retina were removed, the intact pigmented epithelium was separated from the optic cup. Then, RPE was placed in the cell digestion solution (0.08% trypsin-without ethylenediamine tetra-acetic acid + type I collagenase) and incubated at 37°C for 30 minutes. Next, DMEM (10% FBS + 1% penicillin and streptomycin) were used to stop the digestion by pipetting. Next, the solution was spun in a centrifuge at room temperature for three minutes at 800 rpm/min, the cell pellets were resuspended and incubated in a humidified incubator at 5% CO_2 and 37°C.

Investigative Ophthalmology & Visual Science

Transfection and Treatment

Adenovirus overexpressing KAL (Ad-KAL), adenovirus overexpressing Snail (Ad-Snail), and adenovirus overexpressing red fluorescent protein (Ad-CON) were purchased from OBiO (Shanghai, China). MnSOD siRNA (si-MnSOD), Snail siRNA (si-Snail), and non-targeting siRNA (si-CON) were purchased from RiboBio (Guangzhou, China). According to the manufacturer's instructions, the transfection of plasmids was performed at about 70% confluency using Lipofectamine 3000 (L3000015; Gibco). Si-RNA transfection was performed using Lipofectamine RNAiMAX (13778150, Gibco, USA). Recombinant Human TGFβ1 Protein (no. 10804-H08H; Sino Biological Inc., Chesterbrook, PA, USA) was used in 10 ng/mL.

Transwell Assay

Cell vertical migration was determined in a 24-well transwell chamber (26616; Corning, Corning, NY, USA). Cells at 5×10^4 cells/filter in a 200 µL serum-free medium were seeded on cell culture inserts, and 600 µL 20% FBS medium was added to the lower chamber. After being incubated for 16 hours, cells were fixed in ethanol for 20 minutes and stained with 0.1% crystal violet for 10 minutes. Then cells in the upper filter were removed by cotton swabbing, photographed, and counted.

Wound Healing Assay

Cell horizontal migration ability was detected by wound healing assay. The same numbers of cells were seeded in a six-well plate with a complete media. When cells reached 100% confluence, scratched with a 100 µL pipette tip to obtain scratches in a straight line of a constant width and cultured under serum-free media. Cells invading the wound line after 16 hours were photographed with ZEISS Axio Imager Z1 (Zeiss, Jena, Germany) and measured distances to calculate the migration rate.

MnSOD Activity Assay

SOD2 enzymatic activity was assessed using a Cu/Zn-SOD and Mn-SOD assay kit (S0103; Beyotime Institute of Biotechnology, Jiangsu, China) according to the manufacturer's instructions. Add SOD1 inhibitors A and B successively, then incubate with the WST-8/enzyme working solution for 30 min at 37°C. The absorption at 450nm was measured. When the inhibition rate of WST-8 formazan was 50%, the SOD2 enzymatic activity was defined as 1 unit. The protein concentrations for each sample were measured using a BCA assay kit. The results were expressed as unit/µg protein.

Intracellular ROS Levels Assay

Intracellular ROS levels were measured by the ROS assay kit (S0033S; Beyotime Institute of Biotechnology) according to a protocol provided by the manufacturer. Intracellular reactive oxygen species can oxidize non-fluorescent DCFH to produce fluorescent dichlorodihydrofluorescein (DCF). The cells were seeded in a six-well plate (5×10^5 cells/filter). First, we removed the cell culture medium and added an appropriate volume of DCFH-DA diluted with serum-free DMEM at 10 µmol/L. Then, the samples were incubated for 20 minutes at 37°C. Finally, we washed the cells three times with serum-free cell culture mediums. DCF fluorescence was detected by CytoFLEX Flow (Beckman Coulter, Pasadena, CA, USA).

Statistical Analysis

The SPSS 13.0 and GraphPad Prism 8.3 software were used for statistical analysis and data visualization. Mean values were calculated ($n \geq 3$) and presented as mean $\pm$ standard deviation. A *t*-test analysis was performed to compare the two groups. The one-way ANOVA performed multiple groups analysis, then followed by the least significant difference test if the variance was similar between the groups. Moreover, otherwise, the Games-Howell method is required. Statistical significance was considered as a level of $P < 0.05$.

Results

KAL Deficiency Triggers the EMT and Oxidative Stress in RPE During AMD

We used sodium iodate (NaIO3, SI) to generate AMD models to induce retinal cell degeneration, a widely used oxidant specific to RPE cells. Low doses of SI cause the patchy loss of tight junctions in RPE, disrupt outer and inner photoreceptor segments, and cause the accumulation of degradation products of outer photoreceptor segments typical of AMD [19]. We found that thickness increased obviously between RPE and outer/inner segments (OS/IS) (Figs. 1A, 1B), and collagen volume enriched markedly around RPE (Figs. 1C, 1D). At the same time, KAL expression decreased significantly (Figs. 1E, 1F) in SI-induced rats' retinas compared with the control group. Both KAL protein levels and Serpina4 mRNA levels consistently decreased significantly in rats' retinas from the $NaIO_3$ group (Figs. 1G–I). Compelling evidence highlights ROS as crucial conspirators in EMT engagement[18,19] and collagen I promote EMT in multiple diseases.[27] Therefore the results above indicated that KAL might participate in the occurrence of EMT in RPE during AMD.

To verify the causative role of KAL in the RPE dysfunction during AMD, we assessed morphological changes and EMT-related markers in RPE from KAL-KO rats and WT rats separately. It showed that thickness increased obviously in the RPE-OS/IS region from KAL-KO rats (Figs. 1J, 1K) and collagen enriched markedly around RPE compared to WT rats (Figs. 1L, 1M), which confirmed that KAL deprivation led to retinal degeneration. RPE65 is an abundantly expressed protein within the RPE of the eye that is required for retinoid metabolism to support vision.[28] Herein, we stained the retina histological sections with RPE65 monoclonal antibody and found that KAL-KO rats showed lower RPE65 levels in the RPE layer than WT rats (Supplementary Fig. S1A), suggesting KAL loss might also cause RPE dysfunction.

Furthermore, the RPE from KAL-KO SD rats expressed less E-cadherin but more N-cadherin detected by immunofluorescence (Figs. 2A, 2B) and Western blot (Figs. 2C, 2D). RPE cells are usually in resting condition and have no migration function, and the cell migration ability is enhanced when EMT occurs.[29] Therefore we isolated primary RPE cells from rats' retinas and determined them using immunofluorescence (Supplementary Fig. S2). Then, transwell and wound healing assays (Figs. 2E–H) showed that KAL knockout

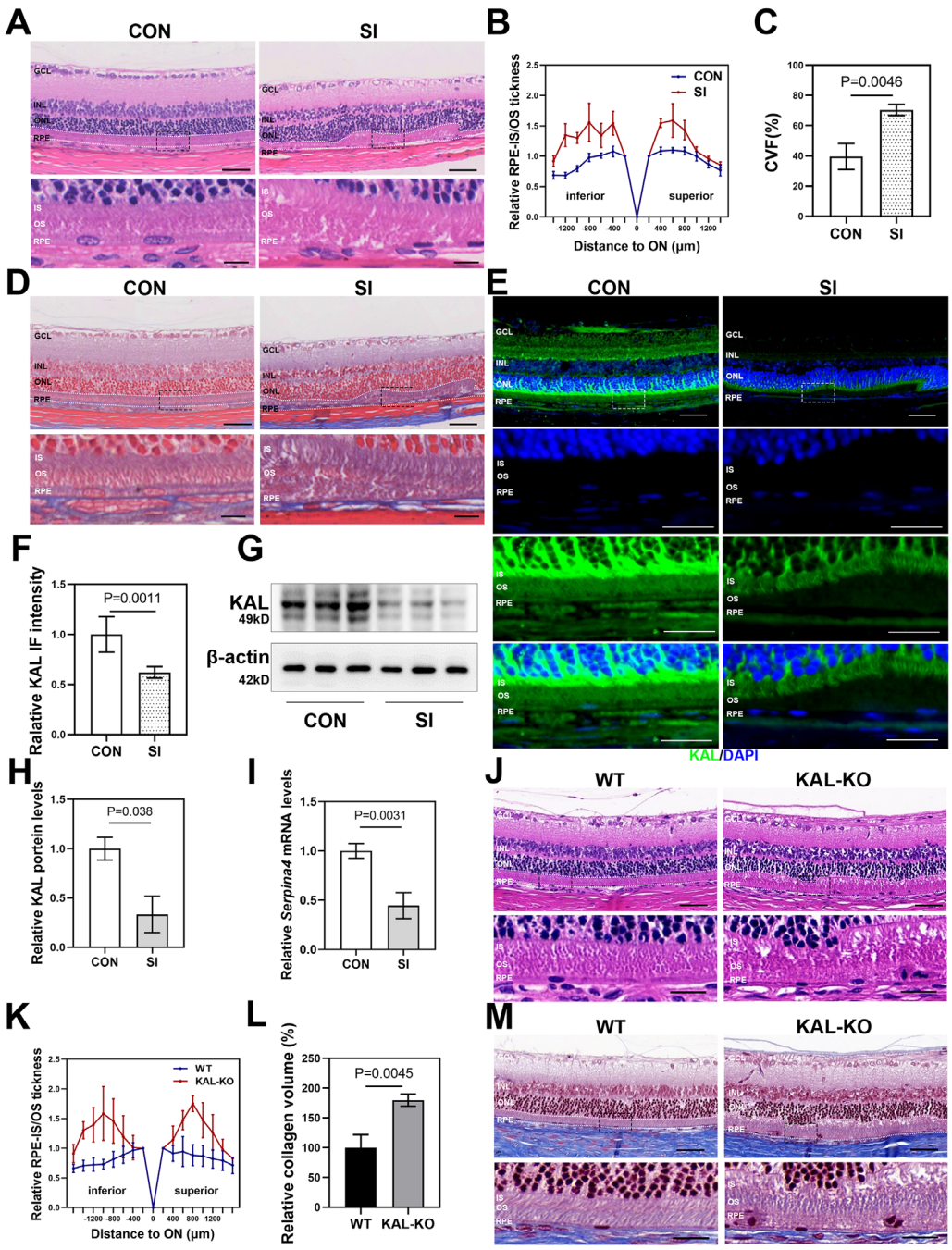

Figure 1. KAL knockout led to AMD-like pathology. **(A)** Representative H&E-stained images of vertical retinal sections from rats showed the morphology in the RPE to IS/OS area marked by the *white dotted line*. Images below are zoomed in from the *black dotted box* showing IS/OS-RPE morphology. **(B)** Quantifying the relative RPE-IS/OS thickness from H&E-stained images of retinal sections from rats. The thickness between RPE and IS/OS is marked as RPE-IS/OS. Measurement at each 200 μm distance to ON and each measurement ratio to the first 200 μm measurement as relative RPE-IS/OS thickness, respectively. (**C, D**) Quantification of CVF and representative Masson-stained images of collagen (*blue*) in the *white dotted line* area from vertical retinal sections from rats. **(E)** Representative immunofluorescence-stained images of vertical retinal sections from rats showed KAL expression (*green*) in retinas. The nuclear was stained with DAPI (*blue*). Images below are zoomed in from the *white dotted box* showing IS/OS-RPE morphology. **(F)** Quantification of relative KAL fluorescence intensity in the regions of IS/OS-RPE. (G-H) Representative Western blot images and quantification of KAL protein levels in rats' retinas. **(I)** The bar graph shows Serpina4 mRNA levels in rats' retinas detected by RT-qPCR. Six-month-old male SD rats received 1% SI in saline at 35 mg/kg or equal volume saline as a control in **A–I**. **(J)** Representative H&E-stained images of vertical retinal sections from WT and KAL-KO rats showed the morphology in the RPE to IS/OS area marked by the *white dotted line*. **(K)** Quantification of the relative RPE-IS/OS thickness from H&E-stained images of retinal sections from WT and KAL-KO rats. **(L, M)** Quantification of CVF and representative Masson-stained images of collagen (*blue*) in the *white dotted line* area from vertical retinal sections from WT and KAL-KO rats. Six-month-old male WT and KAL-KO SD rats were observed in **J–M**. The data are shown as the mean ± S.D and analyzed by *t*-test. *Scale bars:* 50 μm and 10μm in zoom-in images n ≥ 3 per group. CON, control; KAL, Kallistatin; KO, knockout; IS/OS, photoreceptor inner/outer segment; ON, optic nerve; CVF, collagen volume fraction; GCL, ganglion cell layer; INL, inner nuclear layer; ONL, outer nuclear layer; SD, Sprague Dawley. S.D, standard deviation.

Investigative Ophthalmology & Visual Science

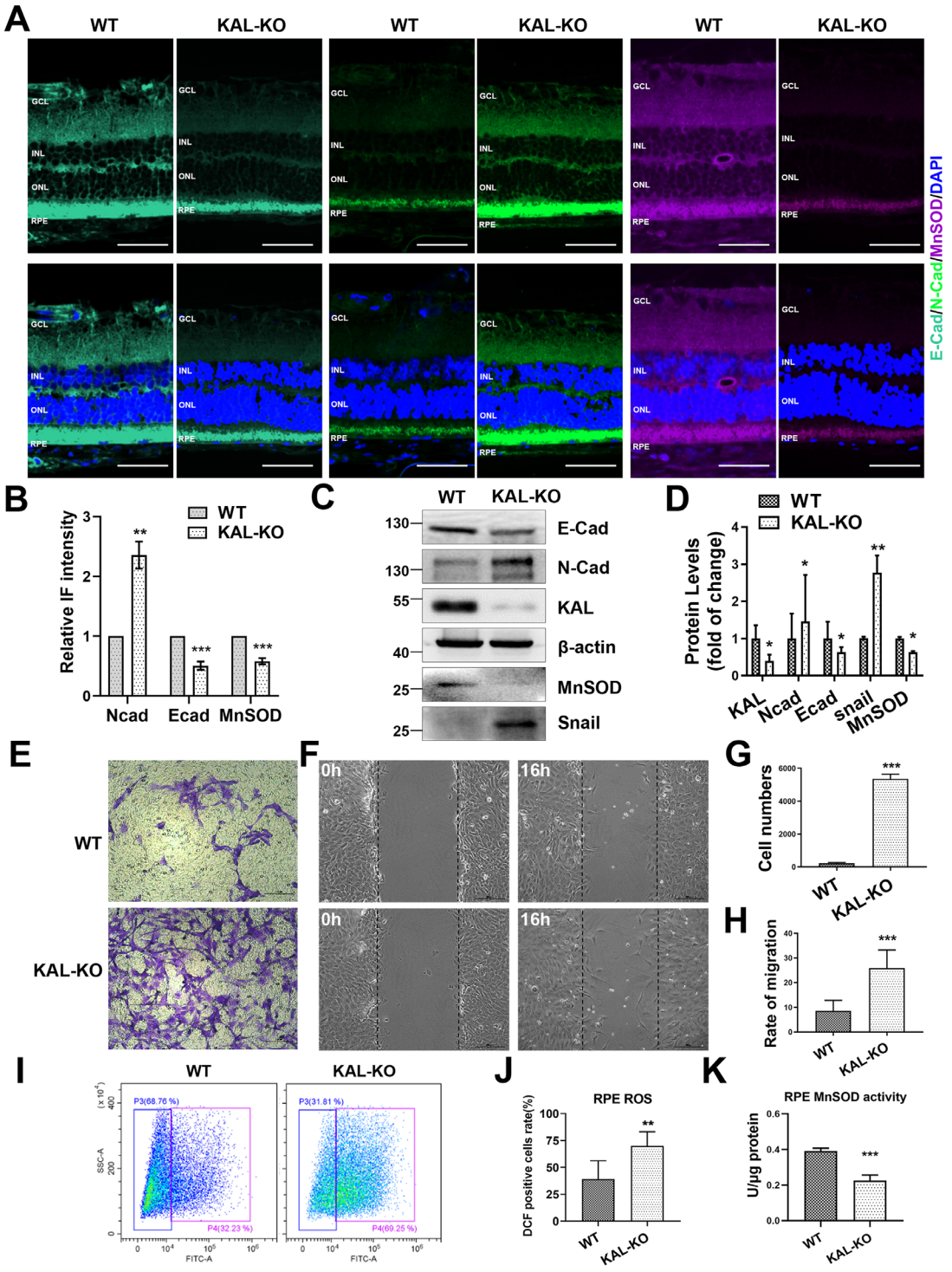

Figure 2. KAL deficiency triggered the EMT and oxidative stress in RPE. **(A)** Representative immunofluorescence images of Ecad (*blue-green*), Ncad (*green*), and MnSOD (*purple*) expression in RPE from rats. The nuclear was stained with DAPI (*blue*). *Scale bars:* 50 μm. **(B)** Quantification of Ecad, Ncad, and MnSOD expression in RPE. **(C)** Western blot analysis of Ecad, Ncad, MnSOD, KAL, and Snail expression in primary RPE cells from rats. **(D)** Bar graphs of quantitative data for protein expression analyzed by Western blot. **(E, F)** Representative images of primary RPE cells from rats were taken at 16 hours after the transwell assay and at 0 hours and 16 hours after the wound healing assay. *Scale bars:* 200 μm. **(G, H)** The histogram of the migrating cell numbers and migration ratio of primary RPE cells in E-F. **(I)** Representative images of intracellular ROS production stained by DCF (x-axis) detected by flow cytometry in primary cells from RPE of rats. **(J)** The histogram of the relative level of intracellular ROS production. **(K)** MnSOD activity in primary cells from RPE rats.6-month-old male WT (n = 3) and KAL-KO (n = 3) SD rats were used in **A–D** and **K**. Two-week-old male WT (n = 4) and KAL-KO (n = 4) SD rats were used in **E–J**. The data are shown as the mean ± S.D. **P* < 0.05, ***P* < 0.01, and ****P* < 0.001 by *t*-test. H&E, hematoxylin and eosin; WT, wild type; RPE, retinal pigment epithelium; IS/OS, photoreceptor inner/outer segment; ON, optic nerve; GCL, ganglion cell layer; INL, inner nuclear layer; ONL, outer nuclear layer; Ecad, E-cadherin; Ncad, N-cadherin; S.D, standard deviation.

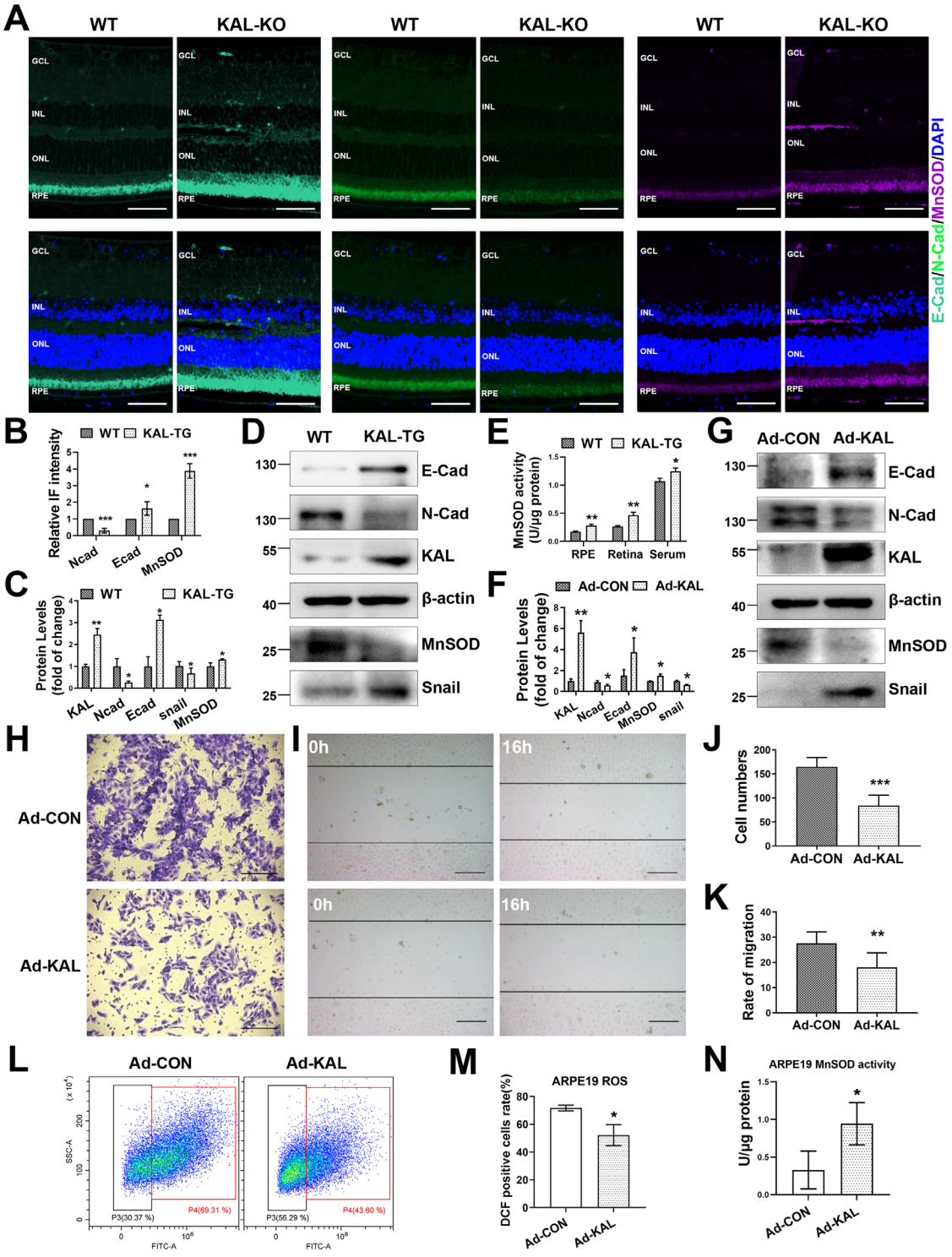

Figure 3. KAL overexpression inhibited the EMT and oxidative stress in RPE. **(A)** Representative immunofluorescence images of Ecad (*blue-green*), Ncad (*green*), and MnSOD (*purple*) expression in RPE from mice. The nuclear was stained with DAPI (*blue*). *Scale bars:* 50 μm. **(B)** Quantitative data of Ecad, Ncad, and MnSOD expression in RPE from mice. **(C, D)** Representative Western blot images and *bar graphs* of quantitative data of Snail, Ecad, Ncad, MnSOD, and KAL expression in RPE from mice. **(E)** MnSOD activity in RPE, retina, and serum from mice. **(F, G)** Representative Western blot images and bar graphs of quantitative data of Ecad, Ncad, MnSOD, Snail, and KAL expression in ARPE19 cells infected with adenovirus overexpressing KAL (Ad-KAL) or control adenovirus (Ad-CON) for 48 hours. **(H, I)** Representative images of the transwell assay (16 hours) and wound healing assay (0 and 16 hours) showed the migrating rate of ARPE19 cells infected with Ad-KAL or Ad-CON for 48 hours. *Scale bars:* 200 μm. **(J, K)** The histogram of the migrating cell numbers and rate of ARPE19 cells infected with Ad-KAL or Ad-CON for 48 hours in **H** and **I**. **(L)** Representative images of intracellular ROS production stained by DCF (x-axis) detected by flow cytometry in ARPE19 cells. **(M)** Quantitative data of intracellular ROS production. **(N)** MnSOD activity in ARPE19 cells infected with Ad-KAL or Ad-CON for 48 hours. Six-month-old WT (n = 5) and KAL-TG (n = 5) C57bl/6J mice were used in **A–E**. Repeat at least three times in **F–N**. The data are shown as the mean ± S.D. **P* < 0.05, ***P* < 0.01, and ****P* < 0.001 by *t*-test. CON, control; Ecad, E-cadherin; Ncad, N-cadherin; S.D, standard deviation.

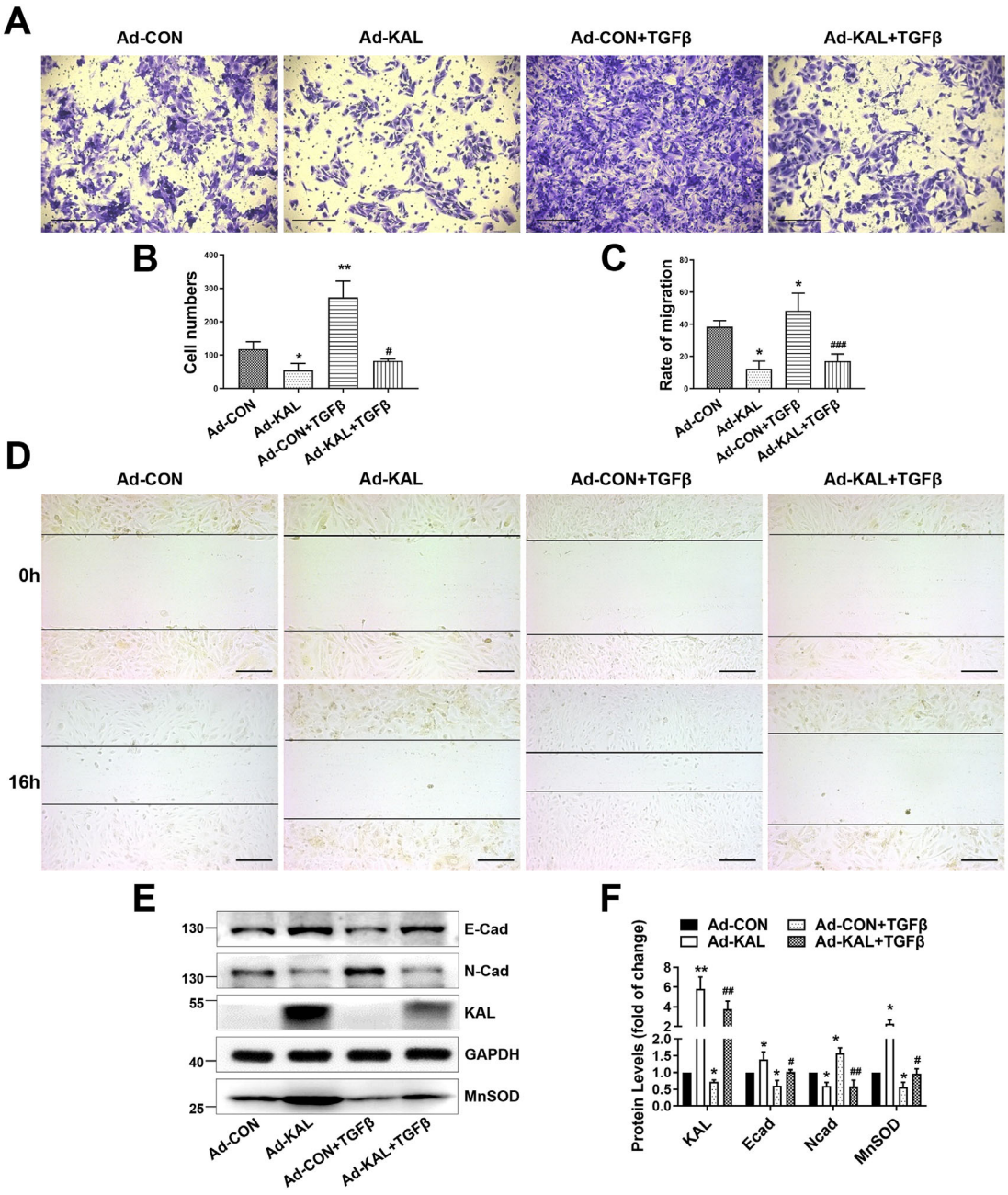

Figure 4. KAL reversed TGFβ-induced EMT and oxidative stress in RPE cells. **(A, B)** Representative images and the histograms of the migrating cell numbers were taken at 16 hours after transwell assay of ARPE19 cells infected by Ad-KAL or Ad-CON for 48 hours with or without TGFβ treatment. **(C, D)** Representative images and the histogram of the migrating rate of ARPE19 cells infected by Ad-KAL or Ad-Con for 48 hours with or without TGFβ were taken at 0 and 16 hours after wound healing. *Scale bars:* 200 µm. **(E)** Western blot detection of MnSOD, Ecad, and Ncad expression in ARPE19 cells infected with Ad-KAL or Ad-CON for 48 hours with or without TGFβ. **(F)** Quantitative data of Western blot detection of MnSOD, Ecad, and Ncad expression in ARPE19 cells infected with Ad-KAL or Ad-CON for 48 hours with or without TGFβ. Repeat at least three times. The data are shown as the mean ± S.D. $^{*}P < 0.05$, $^{**}P < 0.01$, and $^{***}P < 0.001$ versus ARPE19-CON group and $^{\#}P < 0.05$, $^{\#\#}P < 0.01$, and $^{\#\#\#}P < 0.001$ versus ARPE19-CON+TGFβ group by one-way ANOVA test. TGFβ: 10 ng/mL. CON, control; Ecad, E-cadherin; Ncad, N-cadherin; KAL, Kallistatin; S.D, standard deviation.

enhanced the cell migration in primary RPE independent of cell proliferation (Supplementary Fig. S3).

In addition, ROS induced by oxidative stress are involved in the pathological changes of AMD, where MnSOD is a crucial antioxidant enzyme.[20–22] We detected the ROS level in primary RPE cells from WT and KAL-KO rats' retinas to define whether KAL deficiency leads to oxidative stress in RPE. It showed that KAL deficiency significantly increased ROS levels (Figs. 2I, 2J). Furthermore, we found that both MnSOD expression (Figs. 2A–D) and activity (Fig. 2K) in the RPE layer from KAL-KO rats dropped distinctly. These experiments demonstrated that KAL deficiency triggers EMT and oxidative damage in RPE.

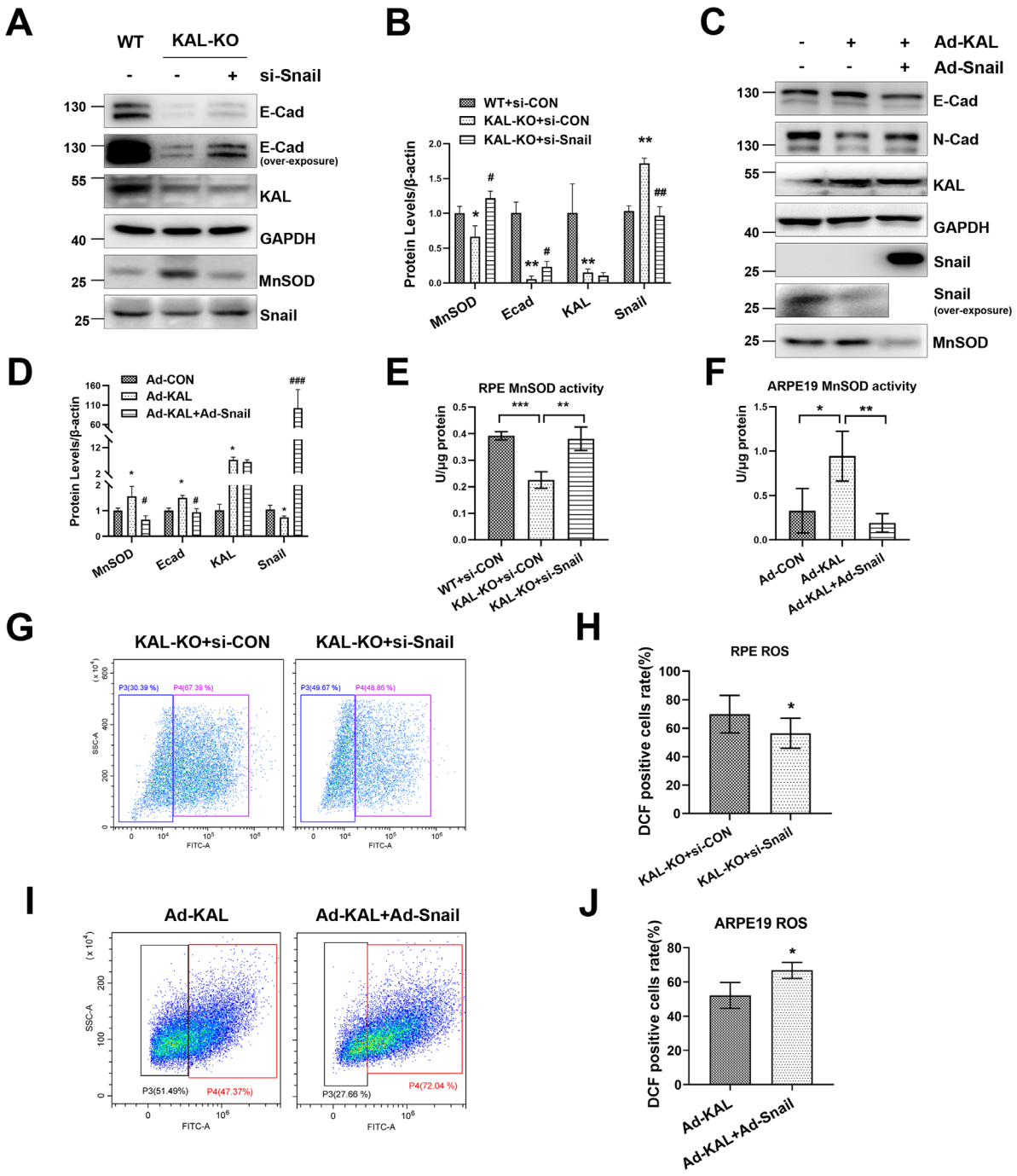

Figure 5. Snail mediated KAL regulating EMT and oxidative stress. **(A)** Representative Western blot images of KAL, MnSOD, Ecad, and Snail expression in primary cells from RPE of rats transfected with Snail small-interference RNA (si-Snail) or control si-RNA (si-CON). **(B)** Quantifying Western blot images of KAL, MnSOD, Ecad, and Snail for **A**. **(C)** Representative Western blot images of KAL, MnSOD, Ecad, Ncad, and Snail in ARPE19 cells infected with Snail adenovirus (Ad-Snail), Ad-KAL, and Ad-CON. **(D)** Quantifying Western blot images of KAL, MnSOD, Ecad, Ncad, and Snail. **(E)** MnSOD activity in primary cells from RPE rats transfected with si-Snail. **(F)** MnSOD activity in ARPE19 cells infected with Ad-KAL or Ad-CON for 48 hours. **(G)** Representative images of intracellular ROS production stained by DCF detected by flow cytometry in primary cells from RPE of rats transfected with si-Snail or si-CON. **(H)** The relative level of intracellular ROS production was analyzed from **G**. **(I, J)** Representative images and quantification data of intracellular ROS production detected by flow cytometry in ARPE19 cells infected with Ad-Snail, Ad-KAL, or Ad-CON. Two-week-old male WT (n = 4) and KAL-KO (n = 4) SD rats were used in **A**, **E**, and **G**. The data are presented as the mean ± S.D. **P* < 0.05, ***P* < 0.01, and ****P* < 0.001 by *t*-test. CON, control; Ecad, E-cadherin; Ncad, N-cadherin; S.D, standard deviation.

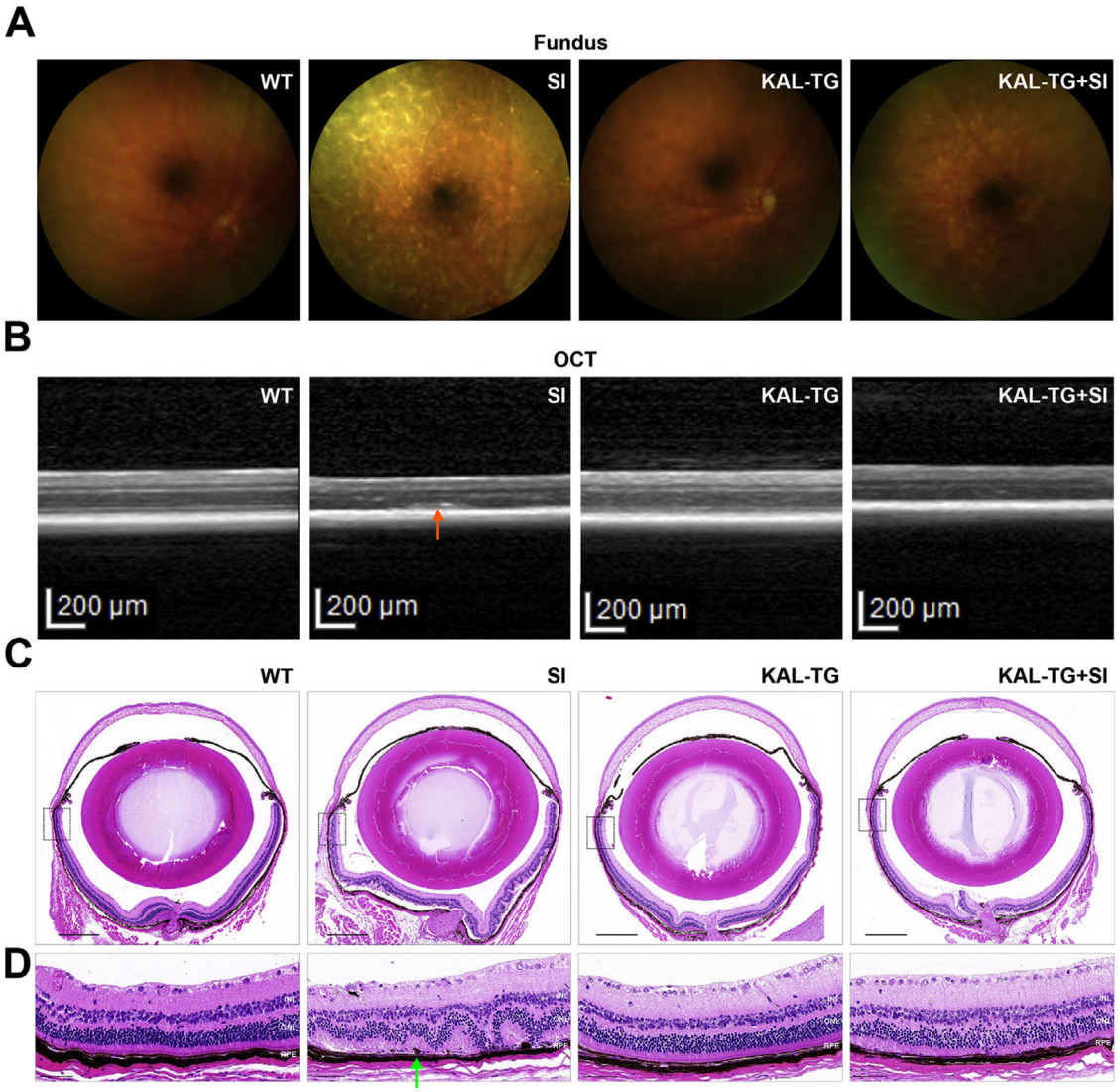

Figure 6. KAL ameliorated sodium iodate-induced AMD-like retinopathy. **(A)** Representative retinal fundus images and **(B)** OCT imaging was performed seven days after injection of SI or saline solution in living mice. The *red arrow* points to lesions in the RPE to IS/OS area. **(C)** Representative full-field H&E-stained images of vertical retinal sections from rats were detected by a bright-field microscope at low magnification. *Scale bars:* 500 μm. Improved areas are marked by the *black box*. **(D)** Zoom-in images from the *black dotted box* in **C** show the RPE morphology in IS/OS area. *Scale bars:* 50 μm. The *green arrow* points to the pigment particles released after RPE destruction. Six-month-old C57BL/6J mice were used (n = 3 per group). IS/OS, photoreceptor inner/outer segment; GCL, ganglion cell layer; INL, inner nuclear layer; ONL, outer nuclear layer.

KAL Overexpression Inhibits the EMT and Oxidative Stress in RPE

To further clarify whether KAL overexpression suppressed the EMT and oxidative damage in RPE cells, we used KAL-TG mice and ARPE19 cells overexpressing KAL with adenovirus. In vivo, KAL overexpression upregulated epithelial marker E-cadherin and repressed mesenchymal marker N-cadherin expression detected by immunofluorescence (Figs. 3A, 3B) and Western blot (Figs. 3C, 3D). In addition, another mesenchymal marker, Fibronectin, also decreased significantly in RPE from KAL-TG mice (Supplementary Figs. S4A, S4B). Moreover, MnSOD expression (Figs. 3A–D) and activity increased notably in RPE, retina, and serum (Fig. 3E) from KAL-TG mice, which indicated that elevated KAL levels might suppress MnSOD-related oxidative stress.

Next, we transfected ARPE19 cells with Ad-KAL or Ad-CON for further experiments in vitro. We found that KAL overexpression promoted epithelial marker E-cadherin expression and muffled mesenchymal marker N-cadherin expression detected by Western blot (Figs. 3F, 3G), besides other mesenchymal markers such as Fibronectin, α-SMA, and MMP9 also decreased significantly in ARPE19 cells transfected with Ad-KAL (Supplementary Figs. S4C, S4D). Furthermore, wound healing and transwell assays (Figs. 3H–K) showed that KAL overexpression suppressed migration ability in ARPE19 cells. Additionally, ARPE19 cells infected with Ad-KAL manifested that intracellular ROS (Figs. 3L, 3M) level declined visibly with enhanced MnSOD expression (Figs. 3F, 3G) and activation (Fig. 3N). In short, these results confirmed that KAL overexpression inhibits the EMT and oxidative stress in RPE cells in vivo and in vitro.

KAL Reverses TGFβ-Induced EMT in RPE Cells

TGFβ is a well-known effective EMT trigger, contributing to AMD development.[23,30] To further clarify the protective role of KAL in TGFβ-induced EMT, ARPE19 cells infected with Ad-KAL or Ad-CON were treated with TGFβ recombinant protein. TGFβ accelerated APRE19 cell migration, but KAL ameliorated this TGFβ-induced migration ability detected by transwell (Figs. 4A, 4B) and wound healing assays (Figs. 4C, 4D). Moreover, Western blot results showed that KAL reversed the reduction of epithelial marker E-cadherin and the upregulation of mesenchymal marker N-cadherin induced by TGFβ (Figs. 4E, 4F). Other mesenchymal markers, such as Fibronectin and Vimentin, exhibited the same trend (Supplementary Fig. S4E-F). Besides, we found that TGFβ reduced MnSOD expression while KAL amended the decline of MnSOD expression in ARPE19 cells (Figs. 4E, 4F). These findings indicated that KAL overexpression reversed TGFβ-induced EMT and protected MnSOD-related oxidative damage in RPE cells.

Snail Mediates KAL Regulating EMT and Oxidative Stress

Another question arises how KAL regulates EMT and oxidative stress of RPE. We found that KAL loss upregulated Snail expression in primary RPE cells from KAL-knockout rats (Fig. 2E-F), and KAL overexpression deterred Snail expression of RPE cells in vivo (Figs. 3C, 3D) and vitro (Figs. 3F, 3G). Because our latest published data demonstrate that Snail transcriptionally regulated MnSOD,[23] and Snail is one crucial transcription factor for EMT.[23,31] Thus we speculated that KAL might regulate EMT and oxidative stress through Snail.

Western blot results showed that Snail interference reversed EMT resulting from KAL scarcity in primary RPE cells from rats (Figs. 5A, 5B). In contrast, Snail overexpression minified the KAL-upregulated E-cadherin expression and distended the KAL-downregulated N-cadherin expression in ARPE19 cells (Figs. 5C, 5D). Furthermore, Snail interference in primary KAL-knockout RPE cells significantly recovered the lower MnSOD activity due to KAL knockdown (Fig. 5E). In comparison, Snail weakened the MnSOD activity promoted by KAL in ARPE19 cells (Fig. 5F). Consequently, Snail loss reduced ROS levels in RPE from KAL knockout rats (Figs. 5G, 5H), and Snail facilitated ROS production in KAL overexpressed ARPE19 cells (Figs. 5I, 5J). These results defined that KAL suppressed oxidative stress-induced EMT via downregulating Snail.

KAL Ameliorates Sodium Iodate-Induced AMD-Like Retinopathy

Fundus photographs showed depigmented patches occupied the whole field of view in $NaIO_3$-induced mice but decreased significantly in KAL transgenic mice (Fig. 6A). Consistently, we found that the RPE layer of mice in the $NaIO_3$ group developed conspicuous high reflex zones detected by OCT (Fig. 6B). Then, we detected retinal histomorphology with H&E staining (Figs. 6C, 6D). It showed a large amount of melanin deposition in the RPE layer retinas of $NaIO_3$-induced mice. The amount of black sediment on the retina in KAL transgenic mice is significantly reduced compared to that in $NaIO_3$-induced mice. Besides, the abnormal shape between RPE-OS/IS became smooth in KAL transgenic mice.

Discussion

For a long time, constructing an animal model of AMD has been an urgent and important goal in ophthalmology research. The spontaneous Rd8 gene frameshift mutation has been found in C57BL/6N and C57BL/6ByJ, leading to abnormal retina pigment epithelium and photoreceptor morphology, but not in any C57BL/6J subline and rat line.[32,33] Besides, intraperitoneal injection of sodium iodate is widely used for generating the AMD model. KAL is well known as antioxidative stress molecular and closely related to retinal diseases. For instance, the level of KAL is significantly reduced in the vitreous cavity of diabetic retinopathy patients[34] and the plasma of AMD patients.[35] Unlike these reports, our study highlights the crucial role of Kallistatin (KAL) on the EMT of RPE in the progress of AMD by using sodium iodate-induced AMD rats and KAL knockout rats. It is accepted that SERPINA4, Serpin family A member 4, encodes KAL, which have been conserved in human, chimpanzee, Rhesus monkey, dog, and rat but not in mouse. Moreover, rat Serpina4 is orthologous to human SERPINA4 (SERPINA4 - Gene - NCBI [nih.gov]). All of these made it a better choice to construct the KAL-KO model using SD rats, not mice lines. Moreover, we observed that KAL-KO rats spontaneously exhibited RPE dysfunction resembling AMD, including the increasing thickness from IS/OS to RPE and oxidative stress-induced EMT in RPE (Figs. 1 and 2) at six months. Thus we provide a valid and phenotypic animal model for AMD research.

The RPE is a monolayer of cells that do not migrate under normal conditions. Ho et al.[36] demonstrated that intraretinal RPE migration is a common occurrence in early to intermediate dry AMD because they found that 61.4% of patients showed intraretinal RPE migration on OCT scans. Moreover, multiple studies showed that RPE cells underwent EMT and allowed RPE cell migration into the retina and the sub-RPE space during AMD.[9,10,37] Thus it's rational that we used transwell assay and wound-healing assay in RPE cells to show RPE migration in the development of AMD. EMT of RPE cells plays a pivotal role in RPE dysfunction disorders, such as diabetic retinopathy,[11] AMD,[6,38,39] and proliferative vitreoretinopathy.[39] The link between KAL and EMT is confined to two studies, which reported that KAL reverses the EMT in the cervical cancer cell[40] and kidney tubular cells.[41] The present study provides new evidence that KAL deficiency initiates EMT using the loss-of-function in the in vivo experiments (Fig. 2). KAL inhibits the EMT of RPE cells in transgenic mice and KAL-overexpressing cells (Fig. 3). RPE cells have multiple physiological functions, like protecting the retina from oxidative stress and phagocytosis of POSs, which are shed daily from retinal photoreceptor cells. In other words, dysfunctional RPE cells failed to remove POSs after losing KAL to resist oxidative stress-induced EMT. These rationally explained that KAL-KO rats showed increased thickness and obvious abnormal histopathology between RPE and OS/IS (Figs. 1J–M). Furthermore, the upregulation of TGFβ plays a critical role in RPE dedifferentiation and promoting EMT in vivo and in vitro.[39,42,43] Subsequently, we further clarify that KAL also protects against TGFβ-induced EMT in RPE (Fig. 4). These results indicate that KAL is vital in initiating EMT in RPE cells, a potential therapeutic target in intraocular disorders related to EMT in RPE, not limited to AMD.

Investigative Ophthalmology & Visual Science

Previous studies reported that KAL increased SOD2 activity, suppressed oxidative stress, and scavenged ROS.[44,45] However, the regulation of KAL on oxidative stress in intraocular diseases remains to be studied. In this study, we found that KAL inhibited EMT of RPE accompanied by enhanced MnSOD expression and activity with less ROS production (Figs. 2 and 3). In addition, we found that si-MnSOD abolished the protective effect of KAL on RPE cells' EMT (Supplementary Fig. S5A, S5B). These data demonstrated that MnSOD was responsible for the inhibitory role of KAL in the EMT of RPE. Moreover, KAL overexpression increased the MnSOD mRNA level even in the cells treated with TGFβ (Supplementary Fig. S5C), which suggested that KAL upregulated MnSOD at the transcription level. Our previous studies have demonstrated that Snail is the critical transcription factor for EMT and mediated the increase of mesenchymal markers induced by high glucose.[46] Our latest published data showed that Snail is a transcriptional repressor for MnSOD, and the Snail-MnSOD axis frames a mutual loop in the development of EMT of RPE.[23] For the first time here, we found that Snail mediated the effect and regulation of KAL, decreasing ROS levels and MnSOD expression and activity (Fig. 5).

The reason for the downregulation of KAL expression in AMD is worthy of further investigation. We have shown that KAL inhibits the EMT induced by TGFβ (Fig. 4). On the other hand, we observed a decreased KAL expression in TGFβ-treated ARPE19 cells even with KAL overexpression (Figs. 4E, 4F). The study of KAL regulation at transcriptional and protein levels is limited. Then we verified that TGFβ negatively regulated the transcription of KAL (Supplementary Figs. S6A–C). We also confirm that TGFβ negatively regulated the transcription of KAL using the Dual-luciferase reporter gene experiment (Supplementary Fig. S6D). Smads are proteins with a transcription factor function, such as EMT responding to TGFβ signaling.[47] First, TGFβ1 binds to the TGFβ membrane receptor, then Smad2 and Smad3 are phosphorylated, form a complex with Smad4, and enter the nucleus to bind with other DNA-binding factors such as Snail to induce EMT. Our subsequent work is worthy of study by the elaborated mechanism by which TGFβ regulated KAL transcription via Smads. Furthermore, we found that Smad3 was phosphorylated in RPE from KAL-KO rats (Supplementary Fig. S6E) and inactivated in RPE from KAL-TG mice and KAL-overexpressed ARPE19 cells (Supplementary Figs. S5F–H). It is reported that KAL prevented fibrosis by inhibiting ROS-induced TGFβ1 expression.[48] Thus it suggests that a feedback loop may be formed between KAL and TGFβ, resulting in a vicious circle of the development of AMD, and the elaborated mechanism is worthy of study in our subsequent work.

It has been well accepted that SI enhanced oxidative damage in the retina to induce the AMD animal model. Here, we found that KAL ameliorated SI-induced AMD-like retinopathy (Fig. 6) in a partial area of the retina. However, we have to note that the improvement appeared in regions far from the optic disk detected by a bright-field microscope at low magnification because of the age of the mice. Therefore we will further use more and younger mice to determine whether KAL relieves the AMD-like pathological changes in all retinas. Furthermore, our team previously discovered that pigmented Brown Norway rats are more prone to severe retinal neovascularization than SD rats in the oxygen-induced retinopathy model.[49,50] Herein, we detected the HIF1α and EVGFA in choroid tissues by Western Blot and found these angiogenesis-related markers did not alter significantly (Supplementary Fig. S7). Thus we can rule out the possibility of KAL's protective role in RPE secondary to vascular stabilization of the choroid.

In conclusion (Supplementary Fig. S8), we obtained evidence that KAL inhibited the oxidative stress-induced EMT in RPE cells by downregulating Snail. Herein, these results offer new insights into the disease mechanisms and may provide a new approach to therapy for dry AMD.

Acknowledgments

The authors thank the staff of the Laboratory Animal Center at State Key Laboratory of Ophthalmology, Zhongshan Ophthalmic Center, for technical support in the OCT examination. We also thank the support from the Advanced Medical Technology Center, The First Affiliated Hospital, Zhongshan School of Medicine, Sun Yat-Sen University.

Supported by The National Natural Science Foundation of China (Grants 82070882, 82070888, 82100917, 82273116, 82203661); Guangdong Special Support Program for Young Top Scientist (Grant 201629046); Guangdong Natural Science Fund (Grant 2023A1515010316, 2021A1515010434, 2022A1515012423, 2022A1515012513); China Postdoctoral Science Foundation (Grant 2021M703679); 2019 Milstein Medical Asian American Partnership Foundation Research Project Award in Translational Medicine.

Disclosure: **G. Shen**, None; **Y. Li**, None; **Y. Zeng**, None; **F. Hong**, None; **J. Zhang**, None; **Y. Wang**, None; **C. Zhang**, None; **W. Xiang**, None; **J. Wang**, None; **Z. Fang**, None; **W. Qi**, None; **X. Yang**, None; **G. Gao**, None; **T. Zhou**, None

References

1. de Jong Paulus TVM. Age-related macular degeneration. *N Engl J Med*. 2006;355:1474.
2. Wong WL, Su X, Li X, et al. Global prevalence of age-related macular degeneration and disease burden projection for 2020 and 2040: a systematic review and meta-analysis. *Lancet Glob Health*. 2014;2:e106.
3. Fleckenstein M, Keenan TDL, Guymer RH, et al. Age-related macular degeneration. *Nat Rev Dis Primers*. 2021;7:31.
4. Strauss O. The retinal pigment epithelium in visual function. *Physiol Rev*. 2005;85:845–881.
5. Somasundaran S, Constable IJ, Mellough CB, Carvalho LS. Retinal pigment epithelium and age-related macular degeneration: a review of major disease mechanisms. *Clin Exp Ophthalmol*. 2020;48:1043–1056.
6. Ghosh S, Shang P, Terasaki H, et al. A role for Ba3/A1-crystallin in type 2 Emt of Rpe cells occurring in dry age-related macular degeneration. *Invest Ophthalmol Vis Sci*. 2018;59:AMD104–AMD113.
7. Datta S, Cano M, Ebrahimi K, Wang L, Handa JT. The impact of oxidative stress and inflammation on Rpe degeneration in non-neovascular Amd. *Prog Retin Eye Res*. 2017;60:201–218.
8. Tamiya S, Liu L, Kaplan HJ. Epithelial-mesenchymal transition and proliferation of retinal pigment epithelial cells initiated upon loss of cell-cell contact. *Invest Ophthalmol Vis Sci*. 2010;51:2755–2763.
9. Radeke MJ, Radeke CM, Shih YH, et al. Restoration of mesenchymal retinal pigmented epithelial cells by Tgfbeta pathway inhibitors: implications for age-related macular degeneration. *Genome Med*. 2015;7:58.
10. Sarks JP, Sarks SH, Killingsworth MC. Evolution of geographic atrophy of the retinal pigment epithelium. *Eye*. 1988;2(Pt 5):552–577.

11. Hirasawa M, Noda K, Noda S, et al. Transcriptional factors associated with epithelial-mesenchymal transition in choroidal neovascularization. *Mol Vis*. 2011;17:1222–1230.
12. Datta S, Cano M, Ebrahimi K, Wang L, Handa JT. The impact of oxidative stress and inflammation on Rpe degeneration in non-neovascular Amd. *Progr Retin Eye Res*. 2017;60:201–218.
13. Kaarniranta K, Uusitalo H, Blasiak J, et al. Mechanisms of mitochondrial dysfunction and their impact on age-related macular degeneration. *Progr Retin Eye Res*. 2020;79:100858.
14. Soundara Pandi SP, Ratnayaka JA, Lotery AJ, Teeling JL. Progress in developing rodent models of age-related macular degeneration (AMD). *Exp Eye Res*. 2021;203:108404.
15. Tisi A, Feligioni M, Passacantando M, Ciancaglini M, Maccarone R. The impact of oxidative stress on blood-retinal barrier physiology in age-related macular degeneration. *Cells*. 2021;10:64.
16. Kaarniranta K, Pawlowska E, Szczepanska J, Jablkowska A, Blasiak J. Role of mitochondrial DNA damage in Ros-mediated pathogenesis of age-related macular degeneration (AMD). *Int J Mol Sci*. 2019;20:2374.
17. Jabbehdari S, Handa JT. Oxidative stress as a therapeutic target for the prevention and treatment of early age-related macular degeneration. *Surv Ophthalmol*. 2020;66:423–440.
18. Chatterjee R, Chatterjee J. ROS and oncogenesis with special reference to EMT and stemness. *Eur J Cell Biol*. 2020;99(2-3):151073.
19. Das TP, Suman S, Damodaran C. Induction of reactive oxygen species generation inhibits epithelial-mesenchymal transition and promotes growth arrest in prostate cancer cells. *Mol Carcinog*. 2014;53:537.
20. Brown EE, DeWeerd AJ, Ildefonso CJ, Lewin AS, Ash JD. Mitochondrial oxidative stress in the retinal pigment epithelium (RPE) led to metabolic dysfunction in both the RPE and retinal photoreceptors. *Redox Biol*. 2019;24:101201.
21. Justilien V, Pang JJ, Renganathan K, et al. *2007, Sod2 Knockdown Mouse Model of Early AMD*. Phildelpha: J. B. Lippincott; 2007:4407.
22. Biswal MR, Han P, Li H, et al. Timing of antioxidant gene therapy: implications for treating dry AMD. *Invest Ophthalmol Vis Sci*. 2017;58:1237–1245.
23. Shen G, Li Y, Hong F, et al. A role for snail-MnSOD axis in regulating epithelial-to-mesenchymal transition markers expression in RPE cells. *Biochem Biophys Res Commun*. 2021;585:146–154.
24. Ma C, Yin H, Zhong J, et al. Kallistatin exerts anti-lymphangiogenic effects by inhibiting lymphatic endothelial cell proliferation, migration and tube formation. *Int J Oncol*. 2017;50:2000.
25. Chao J, Bledsoe G, Chao L. Protective role of kallistatin in vascular and organ injury. *Hypertension*. 2016;68:533–541.
26. Liu X, Zhang B, McBride JD, et al. Antiangiogenic and antineuroinflammatory effects of kallistatin through interactions with the canonical WNT pathway. *Diabetes*. 2013;62:4228–4238.
27. Medici D, Nawshad A. Type I collagen promotes epithelial-mesenchymal transition through ilk-dependent activation of NF-kappaB and LEF-1. *Matrix Biol*. 2010;29:161–165.
28. Kiser PD. Retinal pigment epithelium 65 Kda protein (Rpe65): an update. *Prog Retin Eye Res*. 2022;88:101013.
29. Chtcheglova LA, Ohlmann A, Boytsov D, Hinterdorfer P, Priglinger SG, Priglinger CS. Nanoscopic approach to study the early stages of epithelial to mesenchymal transition (EMT) of human retinal pigment epithelial (RPE) cells in vitro. *Life*. 2020;10:128.
30. Kilinc AN, Han S, Barrett L, Anandasivam N, Nelson CM. Integrin-linked kinase tunes cell-cell and cell-matrix adhesions to regulate the switch between apoptosis and EMT downstream of TGFβ1. *Mol Biol Cell*. 2021;32:402–412.
31. Li H, Li M, Xu D, Zhao C, Liu G, Wang F. Overexpression of snail in retinal pigment epithelial triggered epithelial-mesenchymal transition. *Biochem Biophys Res Commun*. 2014;446:347–351.
32. Mattapallil M, Wawrousek E, Chan C, et al. The Rd8 mutation of the Crb1 gene is present in vendor lines of C57bl/6n mice and embryonic stem cells, and confounds ocular induced mutant phenotypes. *Invest Ophthalmol Vis Sci*. 2012;53:2921–2927.
33. Vessey K, Greferath U, Jobling A, et al. Ccl2/Cx3cr1 knockout mice have inner retinal dysfunction but are not an accelerated model of AMD. *Invest Ophthalmol Vis Sci*. 2012;53:7833–7846.
34. Xing Q, Zhang G, Kang L, et al. The suppression of kallistatin on high-glucose-induced proliferation of retinal endothelial cells in diabetic retinopathy. *Ophthalm Res*. 2017;57:141.
35. Tuo J, Wang Y, Cheng R, et al. Wnt signaling in age-related macular degeneration: human macular tissue and mouse model. *J Transl Med*. 2015;13:330.
36. Ho J, Witkin AJ, Liu J, et al. Documentation of intraretinal retinal pigment epithelium migration via high-speed ultrahigh-resolution optical coherence tomography. *Ophthalmology*. 2011;118:687–693.
37. Shu DY, Butcher E, Saint-Geniez M. EMT and EndMT: emerging roles in age-related macular degeneration. *Int J Mol Sci*. 2020;21:4271.
38. Hyttinen JMT, Kannan R, Felszeghy S, Niittykoski M, Salminen A, Kaarniranta K. The regulation of Nfe2l2 (Nrf2) signalling and epithelial-to-mesenchymal transition in age-related macular degeneration pathology. *Int J Mol Sci*. 2019;20:5800–5800.
39. Zhoui M, Geathers JS, Grillo SL, et al. Role of epithelial-mesenchymal transition in retinal pigment epithelium dysfunction. *Front Cell Dev Biol*. 2020;8:501.
40. Wang T, Shi F, Wang J, Liu Z, Su J. Kallistatin suppresses cell proliferation and invasion and promotes apoptosis in cervical cancer through blocking Nf-κb signaling. *Oncol Res*. 2017;25:809–817.
41. Yiu WH, Li Y, Lok SWY, et al. Protective role of kallistatin in renal fibrosis via modulation of Wnt/B-catenin signaling. *Clin Sci*. 2021;135:429–446.
42. Boles NC, Fernandes M, Swigut T, et al. Epigenomic and transcriptomic changes during human RPE EMT in a stem cell model of epiretinal membrane pathogenesis and prevention by nicotinamide. *Stem Cell Reports*. 2020;14:631–647.
43. Yao H, Ge T, Zhang Y, et al. Bmp7 antagonizes proliferative vitreoretinopathy through retinal pigment epithelial fibrosis in vivo and in vitro. *FASEB J*. 2019;33:3212–3224.
44. Guo Y, Li P, Gao L, et al. Kallistatin reduces vascular senescence and aging by regulating microRNA-34a-SIRT1 pathway. *Aging Cell*. 2017;16:837–846.
45. Yiu WH, Wong DW, Wu HJ, et al. Kallistatin protects against diabetic nephropathy in Db/Db mice by suppressing age-rage-induced oxidative stress. *Kidney Int*. 2016;89:386–398.
46. Che D, Zhou T, Lan Y, et al. High glucose-induced epithelial-mesenchymal transition contributes to the upregulation of fibrogenic factors in retinal pigment epithelial cells. *Int J Mol Med*. 2016;38:1815–1822.
47. David CJ, Huang Y-H, Chen M, et al. TGF-β tumor suppression through a lethal emt. *Cell*. 2016;164:1015–1030.

Investigative Ophthalmology & Visual Science

48. Shen B, Hagiwara M, Yao YY, Chao L, Chao J. Salutary effect of kallistatin in salt-induced renal injury, inflammation, and fibrosis via antioxidative stress. *Hypertension*. 2008;51:1358–1365.
49. Gao G, Li Y, Fant J, Crosson CE, Becerra SP, Ma JX. Difference in ischemic regulation of vascular endothelial growth factor and pigment epithelium–derived factor in Brown Norway and Sprague Dawley rats contributing to different susceptibilities to retinal neovascularization. *Diabetes*. 2002;51:1218–1225.
50. Zhang D, Kaufman PL, Gao G, Saunders RA, Ma JX. Ma Intravitreal injection of plasminogen Kringle 5, an endogenous angiogenic inhibitor, arrests retinal neovascularization in rats. *Diabetologia*. 2001;44:757–765.